Year: 2017

Global field synchronization in gamma range of the sleep EEG tracks sleep depth: Artifact introduced by a rectangular analysis window

Rusterholz, Thomas ; Achermann, Peter ; Dürr, Roland ; Koenig, Thomas ; Tarokh, Leila

DOI: https://doi.org/10.1016/j.jneumeth.2017.04.002

Originally published at:
Rusterholz, Thomas; Achermann, Peter; Dürr, Roland; Koenig, Thomas; Tarokh, Leila (2017). Global field synchronization in gamma range of the sleep EEG tracks sleep depth: Artifact introduced by a rectangular analysis window. Journal of Neuroscience Methods, 284:21-26.
DOI: https://doi.org/10.1016/j.jneumeth.2017.04.002

Global field synchronization in gamma range of the sleep EEG tracks sleep depth: artifact introduced by a rectangular analysis window

Thomas Rusterholz,[*1,2] Peter Achermann,[*1, 3, 4, 5] Roland Dürr,[1] Thomas Koenig,[6] Leila Tarokh[1, 2, 5, 7]

[1]*University of Zurich, Institute of Pharmacology and Toxicology, Zurich, Switzerland*

[2]*University Hospital of Child and Adolescent Psychiatry and Psychotherapy, University of Bern, Bern, Switzerland*

[3]*University of Zurich and ETH Zurich, Neuroscience Center Zurich, Zurich, Switzerland*

[4]*University of Zurich, Zurich Center for Integrative Human Physiology, Zurich, Switzerland*

[5]*University of Zurich, Zurich Center for Interdisciplinary Sleep Research, Zurich, Switzerland*

[6]*University Hospital of Psychiatry Bern, Translational Research Center, University of Bern, Switzerland*

[7]*Department of Psychiatry and Human Behavior, Alpert Medical School of Brown University, Providence, USA*

* equal contributions

Corresponding author:

Prof. Peter Achermann, PhD

Institute of Pharmacology and Toxicology, University of Zurich

Winterthurerstr. 190, CH-8057 Zurich (Switzerland)

Tel : +41 44 63 559 54

Fax : +41 44 63 557 07

Email: acherman@pharma.uzh.ch

Accepted for publication *Journal Neuroscience Methods*, 2017 June 1; 284, 21–26.
DOI 10.1016/j.jneumeth.2017.04.002

Abstract

Background

Investigating functional connectivity between brain networks has become an area of interest in neuroscience. Several methods for investigating connectivity have recently been developed, however, these techniques need to be applied with care. We demonstrate that global field synchronization (GFS), a global measure of phase alignment in the EEG as a function of frequency, must be applied considering signal processing principles in order to yield valid results.

New Method

Multichannel EEG (27 derivations) were analyzed for GFS based on the complex spectrum derived by the fast Fourier transform (FFT). We examined the effect of window functions on GFS, in particular of non-rectangular windows.

Results

Applying a rectangular window when calculating the FFT revealed high GFS values for high frequencies (> 15 Hz) that were highly correlated (r=0.9) with spectral power in the lower frequency range (0.75-4.5 Hz) and tracked the depth of sleep. This turned out to be spurious synchronization. With a non-rectangular window (Tukey or Hanning window) these high frequency synchronization vanished. Both, GFS and power density spectra significantly differed for rectangular and non-rectangular windows.

Comparison with Existing Method(s)

Previous papers using GFS typically did not specify the applied window and may have used a rectangular window function. However, the demonstrated impact of the window function raises the question of the validity of some previous findings at higher frequencies.

Conclusions

We demonstrated that it is crucial to apply an appropriate window function for determining synchronization measures based on a spectral approach to avoid spurious synchronization in the beta/gamma range.

Key words: FFT, GFS, synchronization, spectral analysis

Highlights

- Global field synchronization (GFS) is a global measure of phase alignment applied to the EEG
- We examined the effect of window functions on GFS
- Spurious synchronization occurs in beta/gamma range when using a rectangular window
- Use of appropriate window function is crucial for synchronization measures based on spectral approach

Abbreviations

EEG:	electroencephalogram
FFT:	fast Fourier transform
GFS:	global field synchronization
REM sleep:	rapid eye movement sleep
non-REM sleep:	non-rapid eye movement sleep
SWS:	slow wave sleep (non-REM sleep stages 3 and 4)
SWA:	slow-wave activity (EEG power in 0.625-4.625 Hz range)

1. Introduction

Investigating functional connectivity between brain networks has become a focus in the neurosciences because such measures may capture the exchange and processing of information between networks. Interactions between cortical networks reflect activity-based coupling between brain regions and are critical to brain functioning. Massimini et al. (2005) has demonstrated a breakdown of "effective" cortical connectivity during non- rapid eye movement (non-REM) sleep compared to quiet wakefulness. Thus, the fading of consciousness during sleep may be associated with a breakdown in cortical connectivity.

We aimed to investigate functional connectivity during sleep by estimating global field synchronization (GFS, (Koenig et al., 2001)), a global measure of phase synchronization of multiple EEG channels as a function of frequency. At a given frequency, multichannel EEGs were analyzed for phase alignment between different derivations. GFS ranges from zero (no predominant phase; minimal synchronization) to one (maximal synchronization, all derivations in phase or anti-phase; (Koenig et al., 2001)). The complex spectrum, determined for each EEG derivation with the fast Fourier transform (FFT), is the basis for calculating GFS (see Methods).

By assuming zero time lag between the different EEG channels, we expect that GFS is a measure of global connectivity. We hypothesized that global synchronization would be lower during sleep than waking and that increased synchronization would be observed in the delta and sigma band during non-rapid eye movement (non-REM) sleep. Much to our surprise, our preliminary analysis revealed no clear modulation of GFS by the non-REM-REM sleep cycles at frequencies below 20 Hz. Interestingly, however, GFS in the beta/gamma bands (> 25 Hz; Fig. 1) was modulated by the sleep cycles and showed the highest values during slow wave sleep (N3; SWS, stages 3 and 4). GFS was highly correlated with slow-wave activity (SWA, power in 0.625 - 4.625 Hz range), a marker of sleep intensity, and almost perfectly tracked depth of sleep (Fig. 1 D1). Why would gamma activity be highly synchronized during deep sleep? We were very skeptical about our findings and only through further careful examination of the data set and computational steps did we notice that the manner in which GFS is computed is crucial. Our initial calculation of GFS, which yielded high beta/gamma synchronization during deep sleep, was done with an FFT that used a rectangular window. When we subsequently applied a non-rectangular window functions (e.g., a Tukey or Hanning window) the high gamma synchronization vanished (Fig. 1 D2). We demonstrate in this paper that it is crucial to apply an appropriate window function for determining synchronization measures based on a spectral approach.

A systematic analysis of state dependent GFS changes and the impact of prolonged wakefulness (sleep deprivation) on GFS was reported elsewhere (Achermann et al., 2016).

2. Methods

2.1 Data set

The analyses were performed on an existing dataset of eight healthy young male participants investigating the effects of sleep deprivation on EEG topography (Finelli et al., 2000; Finelli et al., 2001). Polysomnographic recordings were obtained during an adaptation night, a subsequent baseline night, a recovery night after 40 hours of sustained wakefulness, and at 3-h intervals during the 40 h of wakefulness. During baseline and recovery sleep, 27 scalp EEG electrodes (extended 10-20 system; (Finelli et al., 2001; Rusterholz and Achermann, 2011)) were recorded. The analyses of sleep in this paper were restricted to the baseline night. The EEG signals were sampled at 128 Hz (high-pass filter: 0.16 Hz; low-pass filter: 30 Hz; for additional details see (Finelli et al., 2001)). Sleep stages were visually scored for 20-s epochs (C3A2 derivation) according to the standard criteria (Rechtschaffen and Kales, 1968). Artifacts were identified as described in (Finelli et al., 2001). Total sleep time was 446.5 ± 3.6 (SEM) min consisting of 300.5 ± 7.8 min of non-REM sleep (stages 2, 3 and 4) and 103.1 ± 6.9 min of REM sleep (Tinguely et al., 2006). The wake EEG was recorded at 3-h intervals during the period of sleep deprivation (sampling rate: 256 Hz; high-pass filter: 0.16 Hz; low-pass filter: 70 Hz; for additional details see Finelli et al., 2000). Our analysis was restricted to the eyes open condition (4 - 5 min) recorded at 07:00 h after awakening from baseline sleep.

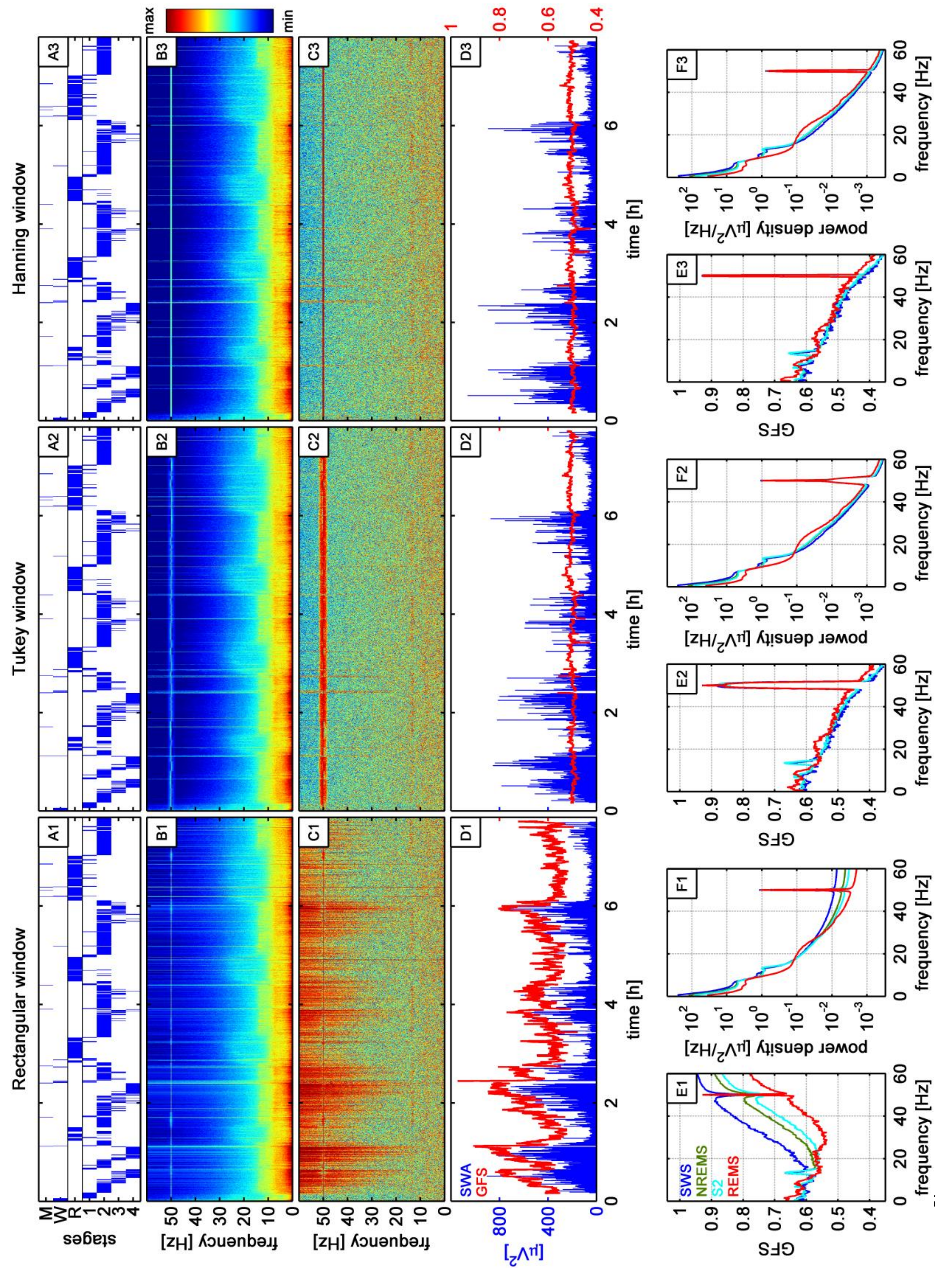

Figure 1: *Global field synchronization (GFS) and spectral power of a baseline night. A1, A2, A3: Hypnogram (20-s epochs; M, movement time; W, waking; REM, REM sleep; 1–4, stages of non-REM sleep). B1, B2, B3: Spectrogram (color-coded power density spectra of 4-s epochs; logarithmic scale, min: -30 dB, max: 25 dB, 0 dB = 1 $\mu V^2/Hz$) of the sleep EEG. C1, C2, C3: Color-coded GFS spectra (4-s epochs; linear scale, min: 0, max: 1). D1, D2, D3: Time course of slow-wave activity (SWA, power in 0.75-4.5 Hz range) and GFS in beta/gamma range (25-45 Hz; smoothed with a moving average filter [21 4-s epochs]). E1, E2, E3: Average GFS spectra of slow wave sleep (SWS; stages 3 and 4), NREM sleep (stages 2, 3 and 4), stage 2 (S2) and REM sleep. F1, F2, F3: Average power density spectra of SWS, NREM sleep, S2 and REM sleep. Left panels with index 1: calculations based on a rectangular window; middle panels with index 2: calculations based on a Tukey window; middle panels with index 3: calculations based on a Hanning window. Power density spectra and SWA are mean values of 27 derivations (average reference).*

2.2 Global field synchronization (GFS)

The estimation of GFS ((Koenig et al., 2001) is briefly summarized here. The EEG was re-referenced to average reference. GFS was computed for consecutive 4-s epochs in the following way: the complex spectrum (Fast Fourier Transform [FFT]) was determined for each derivation yielding a complex value for each frequency and derivation. The complex Fourier coefficients of every channel can be mapped onto the complex plane showing the amplitude and phase of every frequency bin leading to a cloud of points in the complex plane (Fig. 2). The shape of the resulting cloud of points is indicative of the amount of zero-lag phase synchronization across derivations: a very elongated cloud indicates that the EEG at the given frequency is dominated by a common phase or anti-phase across all derivations. In contrast, if the cloud is shaped like a disk, no predominant phase is present. Two-dimensional principal component analysis (PCA) allows quantifying the shape by fitting an elliptical formed bivariate Gaussian distribution where the ratio of the two principal axes correspond to the ratio of the PCA eigenvalues. This was done by calculating the variance-covariance matrix of the real and imaginary part of the Fourier coefficients setting the mean values to zero. The absolute ratio of the difference and sum of the two eigenvalues (λ_1 and λ_2) of this matrix defines the GFS measure:

$$GFS\ (f) = \frac{|\lambda_1(f) - \lambda_2(f)|}{\lambda_1(f) + \lambda_2(f)} \quad (1)$$

GFS ranges from 0 (no predominant phase; minimal synchronization) to 1 (all derivations in phase or anti-phase, maximal synchronization; (Koenig et al., 2001)). A Matlab function to calculate GFS is provided in Supplementary Material.

The FFT was calculated by applying a rectangular window, a Tukey window (tapered cosine; ratio of cosine-tapered section length to the entire window length = 0.2) and a Hanning window (ratio of cosine-tapered section length to the entire window length = 1.0; Fig. 2).

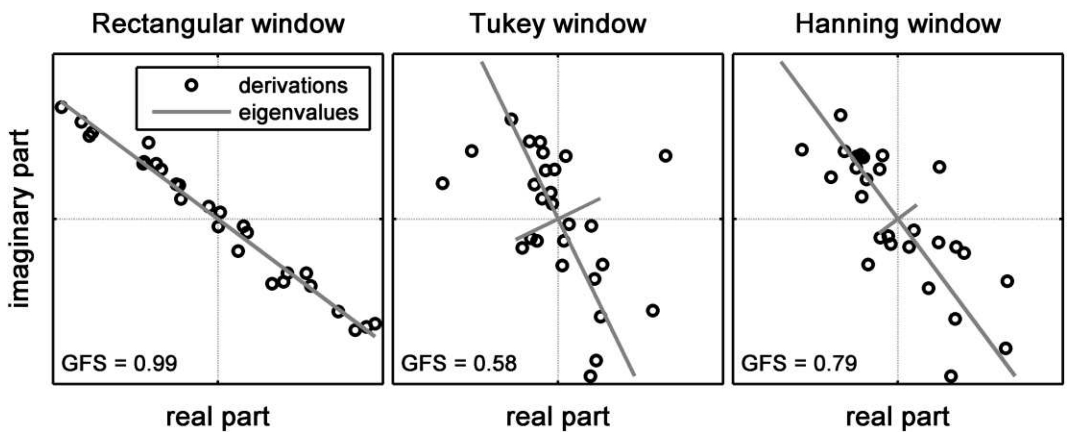

Figure 2: *Illustration of GFS determination in the complex plane for f = 40 Hz (0.25-Hz bin centered at 40 Hz), for a rectangular, a Tukey and a Hanning window (EEG data as in Fig. 3). Black circles: complex Fourier coefficients (one frequency bin) of the 27 derivations of a 4-s epoch. Gray lines: Principal components with relative length of the two eigenvalues.*

2.3 EEG power density spectra

Power density spectra (based on the FFT calculated for determining GFS) were determined for 4-s epochs and matched with sleep stages. A rectangular, a Tukey and a Hanning window (see above) were applied. Spectra were averaged across all 27 derivations (average reference). Additionally, the time course of slow-wave activity (SWA, power in the 0.625 - 4.625 Hz range), a reliable marker of sleep intensity (Achermann and Borbély, 2011), was determined.

Power density and GFS spectra were determined for 4-s epochs resulting in a frequency resolution of 0.25 Hz. Frequency bins are referenced by their mid-frequency (e.g. 2.0 Hz encompassing 1.875 to 2.125 Hz).

2.4 Statistics

For statistical analysis, GFS was Fisher z-transformed and back transformed for illustration.

GFS and power density spectra computed with a rectangular window were compared to spectra computed with the Tukey and Hanning window with a bootstrap analysis. This statistical approach uses a random sample from the original data pool (reshuffling with replacement) and controls the false alarm rate (Maris and Oostenveld, 2007).

3. Results

First, power density and GFS spectra were calculated by applying a rectangular window. We hypothesized that GFS would be highest in the delta and sigma band during non-REM sleep. Such peaks were indeed observed (Fig. 1 E1 and Fig. 4). However, gamma activity in GFS (> 25 Hz; Fig. 1) showed a pronounced modulation by the sleep cycles and highest values during SWS. GFS in this frequency range almost perfectly tracked the depth of sleep as reflected by SWA (Fig. 1 D1). Indeed, GFS in the beta/gamma band (25-45 Hz) was highly correlated with SWA ($r=0.90$; $p<0.001$, both curves smoothed with moving average of 21 4-s epochs; Fig. 1 D1).

GFS calculated with a rectangular window increased as a function of frequency for frequencies > 16 Hz (Fig. 1 E1 and Fig. 4). High GFS in the beta/gamma was an unexpected finding. We wondered, are such high GFS values physiologically meaningful? In animal recordings, beta and gamma activities occur during activated cortical states during waking and REM sleep, and can also be found during the active phases of slow oscillations (Mukovski et al., 2007; Tomofeev, 2012). Similarly, gamma oscillations in humans occur spontaneously during SWS in macroscopic EEG recordings (Valderrama et al., 2012) and might be related to phasic increases in neural activity during slow oscillations. However, somewhat peculiar was the monotonic increase of GFS with increasing frequency.

We speculated that the monotonic increase with increasing frequency might be related to the rectangular window function that was applied to calculate the FFT. Thus, we repeated the analysis by applying a non-rectangular window functions (Fig. 3). Applying such a taper decreases the time series (within a window) to zero or near zero at the beginning and end of the segment in order to avoid sharp discontinuities between the first and last point in periodic time series (read line in top panel of Fig. 3). Therefore, samples in the middle part contribute more to the spectrum. It is implicit to the FFT (or any discrete Fourier transform) that the window analyzed is periodically repeated (Brigham, 1974, 1988). Applying a rectangular function leads to spectral leakage or edge effects, which may be reduced by applying a non-rectangular window function (Harris, 1978).

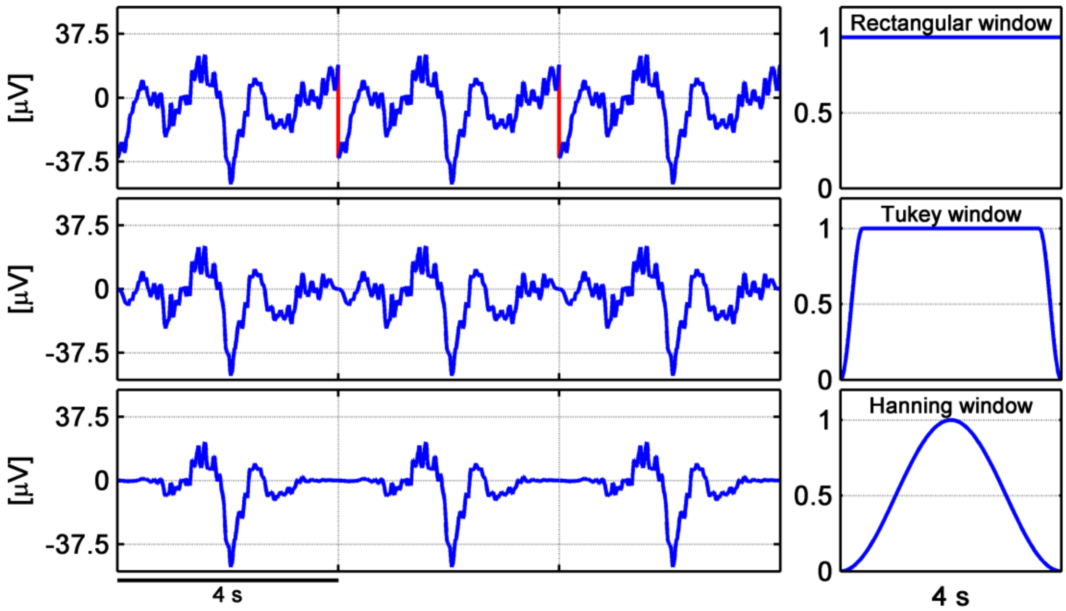

Figure 3: *Effect of window functions. Left panels: EEG signal of a 4-s epoch in sleep stage 4, repeated three times. Edge effect indicated by red lines due to repetition of epochs as implicit in FFT using a rectangular window (upper panel). Removal of edge effect with Tukey and Hanning window (lower panels). Right panels: Comparison of the three window functions.*

Repeating the analysis with a Tukey and a Hanning window (Fig. 3) revealed that GFS no longer increased as a function of frequency for frequencies > 16 Hz (Fig. 1 E2, E3 and Fig. 4). Furthermore, the modulation of GFS in the beta/gamma range by the sleep cycles vanished (Fig. 1 D2, D3).

Figure 2 illustrates the effect of the window function on GFS. Illustrated are the 27 derivations in the complex plane and the resulting first two principal components (λ_1 and λ_2) for a frequency bin of 40 Hz for the 4-s EEG illustrated in Fig. 3. Using a rectangular window, GFS was high due to the edge effect (red line in top panel of Fig. 3) inducing synchronized high frequency components. Applying a Tukey or Hanning window (Fig. 3 lower panels) considerably reduced synchronicity and thus the value of GFS.

A non-rectangular window affects both power density and GFS spectra. Stage specific spectra of an individual are illustrated in Figure 1 (E, F). A statistical comparison of non-REM and REM sleep and wake EEG power density and GFS spectra based on the three windows are provided in Fig. 4. GFS mainly differed between the two windows in the higher frequency range (> 16 Hz for non-REM sleep; > 29 Hz for REM sleep; > 67 Hz for waking; Fig. 4, lower panels) with higher values for a rectangular window, and only to some degree below 16 Hz. Also power density spectra differed in the higher frequency range (> 23 Hz for non-REM sleep; > 33.5 Hz for REM sleep; > 100 Hz for waking; Fig. 4, upper panels) with higher power density for a rectangular window. In contrast to GFS, power density decreased with increasing frequency while GFS steeply increased. Note that the monotonic increase of GFS started below the cut-off frequency of the anti-aliasing low-pass filter and is also observed in the waking EEG sampled with 256 Hz (twice the sampling frequency of the sleep EEG).

In summary, by applying a non-rectangular window, the spurious high synchronization in the beta-gamma frequency range was avoided and a steeper decline of power density with increasing frequency was present.

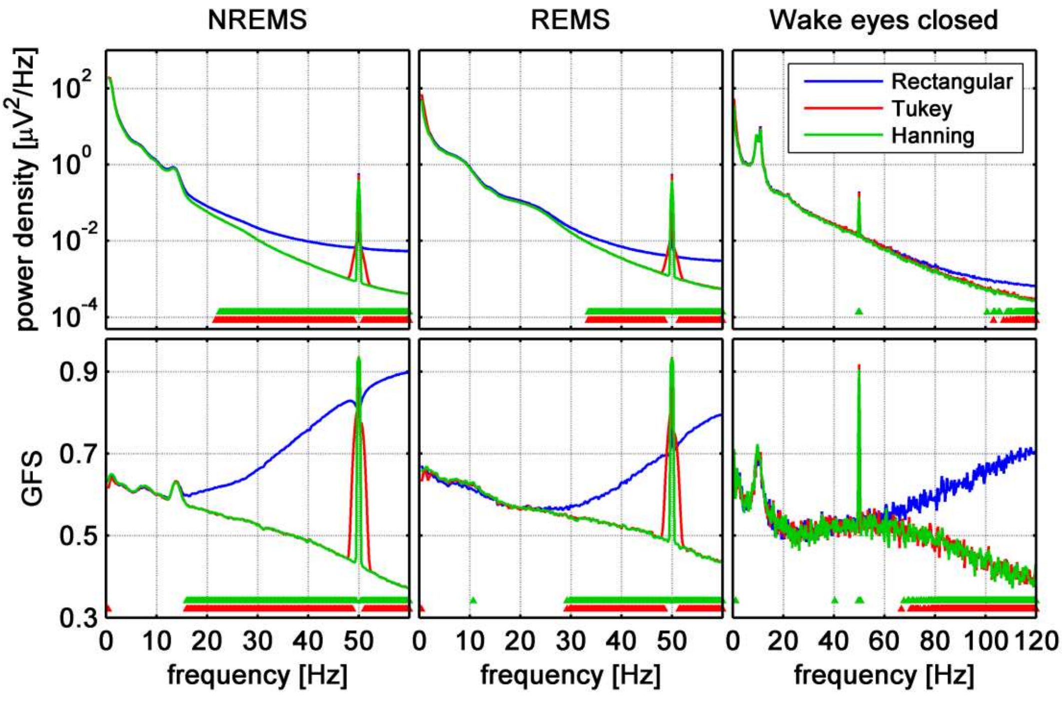

Figure 4: *Average (n=8) power density and GFS spectra calculated with a rectangular, a Tukey and a Hanning window for non-REM (NREM), REM sleep and waking (eyes closed; note the different frequency axis). The spectra of the wake EEG are noisier as they were based on only 4-5 min of data. Differences between the rectangular window and the other two window functions are indicated (▲, p<0.05, bootstrap statistics).*

4. Discussion

We demonstrated that window functions are crucial for spectral analysis of the EEG (and other signals). Both, power density and GFS spectra are strongly dependent on the window function applied (Fig. 4) and differed significantly between rectangular and non-rectangular window functions.

Comparisons of absolute power density spectra determined with different window functions have to be performed with caution as spectra calculated with rectangular and non-rectangular window functions differ significantly (Fig. 4, upper panels). Effects of sleep deprivation on sleep EEG power density spectra, however, are independent of the applied window function, i.e. the frequency range affected by sleep deprivation was independent of the window function (Dijk and Achermann, 1990). Furthermore, the time course of SWA was not affected by the different window functions (Fig. 1, D1, D2, D3) and showed high correlations ($r=0.98$; $p<0.001$, curves not smoothed).

In contrast, GFS spectra calculated with a rectangular window lead to spurious results in the beta/gamma range. We find that GFS monotonically increased with increasing frequency and GFS in the beta/gamma range was highly correlated with SWA. Furthermore, GFS in this frequency range nicely tracked the process of sleep onset (data not shown). After applying a non-rectangular window function with values of zero at the border of the 4-s epochs, those effects disappeared (Fig. 1 and 4). Furthermore, the type of non-rectangular window function seems not to be crucial (Fig. 4). This behavior of GFS with a rectangular window is a consequence of the fact that data offsets at the border of the analysis window (Fig. 3) constitute a broadband and common phase event. In the presence of slow waves, these offsets may be large and thus become the determining constituent of the GFS values obtained in the beta/gamma range. Indeed the effect was most pronounced in non-REM sleep (steepest increase of GFS starting at 16 Hz; Fig. 4), less pronounced in REM sleep and least pronounced for waking. Furthermore, the effect is related to the power-law decline of power density with increasing frequency, as it is typical for EEG data, with highest power always observed in the lowest frequencies. Applying a high pass filter with increasing cut-off frequency reduced or diminished the monotonic increase of GFS in the higher frequencies (Fig. 5). Furthermore, GFS spectra determined with a rectangular window of artificial random data with a power-law characteristic and no phase relationship between the channels also showed a monotonic increase with increasing frequency which disappeared by applying a non-rectangular window function. Thus, the GFS spectra in Figure 1 and 4 obtained with a rectangular window are a superposition of the monotonic GFS increase caused by the edge effect (discontinuity, Fig. 3 top panel) and real physiological synchronization present in the lower frequency range (< 16 Hz). A further contributing factor is the epoch length applied to calculate the FFT. Longer epochs led to a less pronounced monotonic increase of GFS in the higher frequencies. With longer epochs, however, one has to face the problem of non-stationarity of the signal. Four- to 5-s epochs are a good compromise to have quasi-stationary signals for spectral analysis.

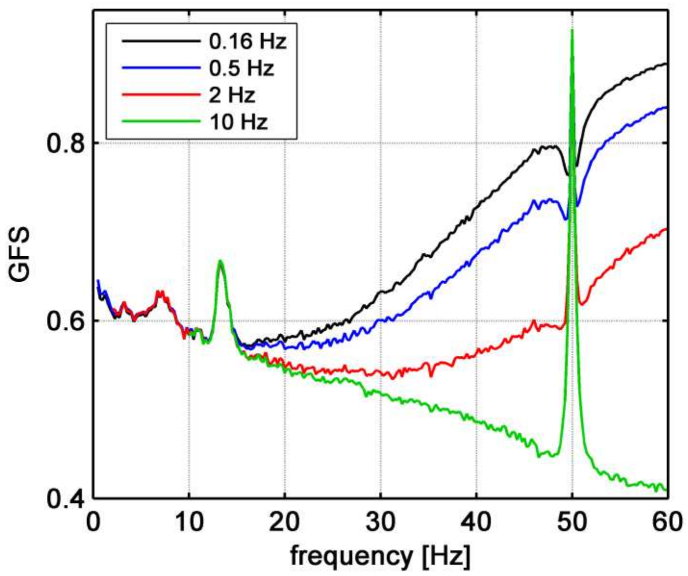

Figure 5: *Average GFS spectra of NREM sleep (stages 2, 3 and 4; same subject as in Fig. 1) calculated with a rectangular window after applying a high-pass filter with different cut-off frequencies: 0.16 Hz (original recording), 0.5 Hz, 2 Hz and 10 Hz.*

Many previous papers using GFS have not specified the applied window function (Kikuchi et al., 2007; Koenig et al., 2001; Koenig et al., 2005; Ma et al., 2014; Michels et al., 2012; Nicolaou and Georgiou, 2014; Park et al., 2008; Pugnetti et al., 2010). Our finding of the importance of the windowing function on the GFS values at higher frequencies raises the question of the validity of some previous findings at higher frequencies and stresses the need of providing details of the applied methodology.

Conclusion: Synchronization measures based on a spectral approach (FFT) depend on the applied window function, in particular for frequencies above 15 Hz. Thus, it is crucial to use a non-rectangular window function to avoid spurious high synchronization in the beta-gamma frequency range.

5. Acknowledgements

We thank Antonio Fernandez Guerrero for fruitful discussions on the interpretation of GFS. The study was supported by the Swiss National Science Foundation grant 32003B_146643 and CRSII3_136249. The funders had no role in study design, data collection and analysis, decision to publish, or preparation of the manuscript.

The authors declare nor conflict of interest.

6. References

Achermann P, Borbély AA. Sleep homeostasis and models of sleep regulation. In Kryger MH, Roth T, Dement WC, editors. Principles and Practice of Sleep Medicine. Elsevier Saunders: Missouri, 2011: 431- 44.

Achermann P, Rusterholz T, Dürr R, Koenig T, Tarokh L. Global field synchronization reveals rapid eye movement sleep as most synchronized brain state in the human EEG. R. Soc. open sci., 2016; 3: 160201.

Brigham EO. The Fast Fourier Transform. Prentice-Hall Inc: Englewood Cliffs, New Jersey, 1974.

Brigham EO. The Fast Fourier Transform and Its Applications. Prentice-Hall Inc: Englewood Cliffs, New Jersey, 1988.

Dijk DJ, Achermann P. Window functions affect power spectra of human sleep EEGs significantly, but not substantially. Abstracts of the 10th Congress of the European Sleep Research Society: Strasbourg, 1990.

Finelli LA, Baumann H, Borbely AA, Achermann P. Dual electroencephalogram markers of human sleep homeostasis: correlation between theta activity in waking and slow-wave activity in sleep. Neuroscience, 2000; 101: 523-9.

Finelli LA, Borbély AA, Achermann P. Functional topography of the human nonREM sleep electroencephalogram. European Journal of Neuroscience, 2001; 13: 2282-90.

Harris FJ. On the use of windows for harmonic analysis with the discrete Fourier transform. Proceedings of the IEEE, 1978; 66: 51-83.

Kikuchi M, Koenig T, Wada Y, Higashima M, Koshino Y, Strik W, Dierks T. Native EEG and treatment effects in neuroleptic-naive schizophrenic patients: Time and frequency domain approaches. Schizophrenia Research, 2007; 97: 163-72.

Koenig T, Lehmann D, Saito N, Kuginuki T, Kinoshita T, Koukkou M. Decreased functional connectivity of EEG theta-frequency activity in first-episode, neuroleptic-naive patients with schizophrenia: preliminary results. Schizophr Res, 2001; 50: 55-60.

Koenig T, Prichep L, Dierks T, Hubl D, Wahlund LO, John ER, Jelic V. Decreased EEG synchronization in Alzheimer's disease and mild cognitive impairment. Neurobiology of Aging, 2005; 26: 165-71.

Ma C-C, Liu A-J, Liu A-H, Zhou X-Y, Zhou S-N. Electroencephalogram Global Field Synchronization Analysis: A New Method for Assessing the Progress of Cognitive Decline in Alzheimer's disease. Clinical Eeg and Neuroscience, 2014; 45: 98-103.

Maris E, Oostenveld R. Nonparametric statistical testing of EEG- and MEG-data. J Neurosci Methods, 2007; 164: 177-90.

Massimini M, Ferrarelli F, Huber R, Esser SK, Singh H, Tononi G. Breakdown of cortical effective connectivity during sleep. Science, 2005; 309: 2228-32.

Michels L, Luechinger R, Koenig T, Martin E, Brandeis D. Developmental Changes of BOLD Signal Correlations with Global Human EEG Power and Synchronization during Working Memory. Plos One, 2012; 7.

Mukovski M, Chauvette S, Timofeev I, Volgushev M. Detection of active and silent states in neocortical neurons from the field potential signal during slow-wave sleep. Cereb Cortex, 2007; 17: 400-14.

Nicolaou N, Georgiou J. Global field synchrony during general anaesthesia. Br J Anaesth, 2014; 112: 529-39.

Park Y-M, Che H-J, Im C-H, Jung H-T, Bae S-M, Lee S-H. Decreased EEG synchronization and its correlation with symptom severity in Alzheimer's disease. Neuroscience Research, 2008; 62: 112-7.

Pugnetti L, Baglio F, Farina E, Alberoni M, Calabrese E, Gambini A, Di Bella E, Garegnani M, Deleonardis L, Nemni R. EEG Evidence of Posterior Cortical Disconnection in PD and Related Dementias. International Journal of Neuroscience, 2010; 120: 88-98.

Rechtschaffen A, Kales A. A manual of standardized terminology, techniques and scoring system for sleep stages of human subjects. National Institutes of Health: Bethesda, Maryland, 1968.

Rusterholz T, Achermann P. Topographical aspects in the dynamics of sleep homeostasis in young men: individual patterns. BMC Neurosci, 2011; 12: 84.

Tinguely G, Finelli LA, Landolt HP, Borbely AA, Achermann P. Functional EEG topography in sleep and waking: state-dependent and state-independent features. Neuroimage, 2006; 32: 283-92.

Tomofeev I. Neuronal Oscillation in the Thalamocortical System during Sleeping and Waking States. In Frank MG, editor. Sleep and Brain Activity. Academic Press: Oxford, 2012: 1-21.

Valderrama M, Crepon B, Botella-Soler V, Martinerie J, Hasboun D, Alvarado-Rojas C, Baulac M, Adam C, Navarro V, Le Van Quyen M. Human Gamma Oscillations during Slow Wave Sleep. PloS One, 2012; 7: e33477.